Observation of the Isovector Giant Monopole Resonance via the ^{28}Si(^{10}Be,^{10}B^{*}[1.74 MeV]) Reaction at 100 AMeV

M. Scott *et al.*

Phys. Rev. Lett. **118**, 172501 — Published 28 April 2017

DOI: 10.1103/PhysRevLett.118.172501

Observation of the Isovector Giant Monopole Resonance via the ^{28}Si(^{10}Be,^{10}B*[1.74 MeV]) reaction at 100 AMeV

M. Scott,[1,2,3] R.G.T. Zegers,[1,2,3,*] R. Almus,[4] Sam M. Austin,[1,2,3] D. Bazin,[1] B.A. Brown,[1,2,3] C. Campbell,[5] A. Gade,[1,3] M. Bowry,[1] S. Galès,[6,7] U. Garg,[8] M.N. Harakeh,[9] E. Kwan,[1] C. Langer,[1,2] C. Loelius,[1,2,3] S. Lipschutz,[1,2,3] E. Litvinova,[10,1,2] E. Lunderberg,[1,3] C. Morse,[1,3] S. Noji,[1,2] G. Perdikakis,[4,1,2] T. Redpath,[4] C. Robin,[10,2] H. Sakai,[11] Y. Sasamoto,[12,11] M. Sasano,[11] C. Sullivan,[1,2,3] J.A. Tostevin,[13,1] T. Uesaka,[11] and D. Weisshaar[1]

[1]*National Superconducting Cyclotron Laboratory, Michigan State University, East Lansing, Michigan 48824, USA*
[2]*Joint Institute for Nuclear Astrophysics, Michigan State University, East Lansing, Michigan 48824, USA*
[3]*Department of Physics and Astronomy, Michigan State University, East Lansing, Michigan 48824, USA*
[4]*Department of Physics, Central Michigan University, Mount Pleasant, Michigan 48859, USA*
[5]*Lawrence Berkeley National Laboratory, Berkeley, California 94720, USA*
[6]*IPN Orsay, CNRS-IN2P3, Université Paris-Sud, Université Paris-Saclay, 91406 Orsay Cedex, France*
[7]*Horia Hulubei National Institute of Physics and Nuclear Engineering, P.O. Box MG6, Bucharest, Romania*
[8]*Department of Physics, University of Notre Dame, Notre Dame, IN 46556, USA*
[9]*Kernfysisch Versneller Instituut - Center for Advanced Radiation Technology, University of Groningen, Groningen, 9747 AA, The Netherlands*
[10]*Department of Physics, Western Michigan University, Kalamazoo, MI 49008-5252, USA*
[11]*RIKEN, Nishina Center, Wako, 351-0198, Japan*
[12]*Center for Nuclear Study, University of Tokyo, RIKEN Campus, Wako, Saitama 351-0198, Japan*
[13]*Department of Physics, University of Surrey, Guilford, Surrey GU2 7XH, United Kingdom*

(Dated: March 6, 2017)

The (^{10}Be,^{10}B*[1.74 MeV]) charge-exchange reaction at 100 AMeV is presented as a new probe for isolating the isovector ($\Delta T = 1$) non-spin-transfer ($\Delta S = 0$) response of nuclei, with ^{28}Si being the first nucleus studied. By using a secondary ^{10}Be beam produced by fast fragmentation of ^{18}O nuclei at the NSCL Coupled Cyclotron Facility, applying the dispersion-matching technique with the S800 magnetic spectrometer to determine the excitation energy in ^{28}Al, and performing high-resolution γ-ray tracking with the Gamma-Ray Energy Tracking Array (GRETINA) to identify the 1022-keV γ ray associated with the decay from the 1.74-MeV $T = 1$ isobaric analog state in ^{10}B, a $\Delta S = 0$ excitation-energy spectrum in ^{28}Al was extracted. Monopole and dipole contributions were determined through a multipole-decomposition analysis, and the isovector giant dipole (IVGDR) and monopole (IVGMR) resonances were identified. The results show that this probe is a powerful tool for studying the elusive IVGMR, which is of interest for performing stringent tests of modern density functional theories at high excitation energies and for constraining the bulk properties of nuclei and nuclear matter. The extracted distributions were compared with theoretical calculations based on the normal-modes formalism and the proton-neutron relativistic time-blocking approximation. Calculated cross sections based on these strengths underestimate the data by about a factor of two, which likely indicates deficiencies in the reaction calculations based on the distorted wave Born approximation.

PACS numbers: 24.30-v, 25.60.Lg, 25.70.Kk, 21.60.Jz

The isovector giant monopole resonance (IVGMR) is of interest as a collective phenomenon in nuclei at high excitation energies. It can be described as a breathing mode in which the proton and neutron density distributions oscillate out of phase[1]. Consequently, similar to its isoscalar partner, the isoscalar giant monopole resonance (ISGMR) [2–4], the IVGMR can be used to gain a better understanding of the bulk properties of nuclei and nuclear matter if high-quality data were available [5, 6]. The excitation energy of the IVGMR is sensitive to the surface and volume symmetry energy coefficients [7] and a systematic study over a wide target mass range provides an additional method to constrain these quantities, which are key for understanding the properties of asymmetric nuclear matter, including neutron stars [8]. Furthermore, the non-energy-weighted sum rule for the IVGMR depends sensitively on the differences between radii of the neutron and proton distributions in nuclei [5]. Hence, detailed information about the strength distribution of the IVGMR provides a tool to better understand the properties of neutron skins, from which the density dependence of the symmetry energy for asymmetric nuclear matter can be constrained [9, 10]. In a microscopic description, the IVGMR is an excitation of the nucleus that is a coherent superposition of one-particle one-hole ($1p$-$1h$) excitations across a major oscillator shell ($2\hbar\omega$),

* zegers@nscl.msu.edu

characterized by no change in the orbital angular momentum ($\Delta L = 0$), no change of spin $\Delta S = 0$, and a change in isospin of one unit ($\Delta T = 1$) [1, 5]. It has been postulated to mediate isospin-symmetry breaking and isospin mixing [6, 11–13]. More generally, measurements of the properties of the IVGMR serve as a stringent test of microscopic models of nuclei at high excitation energies [14].

Because the excitation of spin-transfer partner of the IVGMR, the isovector spin giant monopole resonance (IVSGMR), is much stronger at intermediate beam energies ($E > 50$ AMeV) [15–22], evidence for the IVGMR has only been found by using CE reactions that are selective of $\Delta S = 0$ excitations. In pion CE reactions [23–25], excess strength at forward scattering angles was associated with the excitation energy of the IVGMR. However, the large width of the IVGMR (10–15 MeV) and the contribution of a strong non-resonant continuum component in the spectrum at high excitation energies significantly hampered the analysis. Evidence for the IVGMR was also reported in a study of the ^{60}Ni(^{7}Li,^{7}Be+γ) [26] reaction at 65 AMeV, in which the coincidence with the γ decay from the excited 430-keV state in ^{7}Be allows for the isolation of the excitation-energy spectrum associated with $\Delta S = 1$ transitions. The spectrum for $\Delta S = 0$ is then generated by subtracting the $\Delta S = 1$ spectrum from the total spectrum. In addition to the uncertainties related to this subtraction procedure, the results also relied strongly on the description of the continuum. Nevertheless, since the transition densities of the isovector monopole resonances have a node near the nuclear surface, a heavy-ion CE probe could be advantageous for studying the IVGMR. Heavy-ion probes are strongly absorbed near the nuclear surface and a cancelation of amplitudes from the nuclear interior and surface portions of the transition density is avoided [27, 28].

In this Letter, we show that the (^{10}Be,^{10}B*[1.74 MeV]) CE reaction at E(^{10}Be)=100 AMeV is a new tool for isolating $\Delta S = 0$ strength and studying the IVGMR. As described below, by selecting the ejected ^{10}B in coincidence with the 1.022-MeV γ ray from the transition of the superallowed Fermi transition ^{10}Be(0^+, g.s.)$\rightarrow$^{10}B($0_1{}^+$, 1.74 MeV, T=1) to the ^{10}B($1_1{}^+$, 0.718 MeV) level, a $\Delta S = 0$, $\Delta T = 1$ filter is obtained.

Since ^{10}Be was produced as a secondary low-intensity, beam from in-flight fragmentation, a light target nucleus (^{28}Si) was chosen for this first investigation since the cross sections decrease rapidly with increasing target mass. At an energy of 100 AMeV, the reaction mechanism is well described as a single-step direct process [29], and it is possible to perform a multipole-decomposition analysis (MDA) to separate excitations associated with different multipolarities. The present experiment was inspired by an earlier study that used the (^{10}C,^{10}B+γ) reaction [30], which is the $\Delta T_z = -1$ mirror of the (^{10}Be,^{10}B+γ) reaction. The earlier experiment was hampered by the relatively poor resolution of the γ energy after Doppler reconstruction, which resulted in a poor signal-to-noise ratio for the 1.022-MeV peak. By using the HPGe GRETINA array [31, 32] in the present experiment, the signal-to-noise ratio is greatly improved.

A 150-pnA, 120 AMeV beam of ^{18}O from the NSCL coupled-cyclotron facility (CCF) [33] struck a 1000-mg/cm^2 thick Be target at the entrance of the A1900 fragment separator [34]. The beam line to the S800 target was operated in dispersion-matched ion optics [35]. A ^{10}Be beam (98% pure) with a rate of $\sim 7 \cdot 10^6$ particles per second and an average energy of 100 AMeV (with a momentum spread of $\pm 0.25\%$) was transported to a 150-μm thick ^{nat}Si wafer (92.22% ^{28}Si) placed at the target of the S800 spectrometer [36]. Besides ^{nat}Si, data were also taken on a ^{nat}C target (98.88% ^{12}C) to test the effectiveness of the (^{10}Be,^{10}B+γ) probe for removing $\Delta S = 1$ contributions from the excitation-energy spectra.

^{10}B reaction products were momentum analyzed in the S800 spectrograph [36], and detected in the focal plane by two cathode-readout drift chambers (CRDCs), an ionization chamber, and a plastic scintillator [37]. Particle identification was performed by measuring the time of flight to the scintillator relative to the CCF RF signal, and the energy loss signal in the ionization chamber. From the positions measured in the CRDCs, the angles and momenta of the ^{10}B tracks were reconstructed. Excitation energies of the residual ^{28}Al ions were obtained in a missing-mass calculation with a resolution of 2.2 MeV (FWHM). Scattering angles were measured for $0 \leq \theta_{lab} \leq 5^\circ$ with a resolution of 0.5° (FWHM).

The γ-rays from the de-excitation of the ^{10}B reaction product are emitted in-flight. Doppler reconstruction is required to determine the γ energy in the rest frame of ^{10}B, which benefits strongly from the accurate measurement of the angle and energy of the γ rays in GRETINA [31, 32]. The detection efficiency and reconstructed energy resolution for the 1.022-MeV γ ray in ^{10}B were $5.06 \pm 0.05\%$ and 20 keV, respectively.

Fig. 1(a) shows the Doppler-reconstructed γ-ray spectrum taken with the ^{nat}C target and the inset shows the relevant part of the level diagram in ^{10}B. The peak at 1.022 MeV is from the decay of the 1.74 MeV 0^+ T=1 state to the 0.718-MeV 1^+ state, and by gating on this peak, a $\Delta S = 0$ filter is created. Contributions from background events under the 1.022 MeV peak were estimated and subtracted by using a sideband at energies just above the 1.022-MeV peak. The signal-to-noise ratio for the peak in gate I was 1.5 (for the case of the ^{28}Si target discussed below, the signal-to-noise ratio was 1.1). The yield from the sideband was scaled to match the estimated background under the peak. The broad peak at ~ 0.7 MeV originates from the decay of the 0.718-MeV 1^+ state to the ground state. It is broad because its half-life is 0.71 ns and the decay occurs over an extended distance after the target, thereby distorting the γ-ray angle measurement and Doppler reconstruction. By gating on this peak, $\Delta S = 1$ events (from reactions that directly populate this state) and $\Delta S = 0$ events (from

feeding through the 1.74-MeV 0^+ state) are selected. A sideband background subtraction procedure was also carried out by using events just above this peak, but it has relatively large uncertainties because the signal is broad. Finally, a smaller peak was observed at 0.41 MeV. It arises from the de-excitation of the 2.15-MeV 1^+ state, which has a 52% probability of feeding the 1.74-MeV 0^+ state [38]. As it contaminated the $\Delta S = 0$ filter, events gated on this transition were also analyzed by using a sideband subtraction, so that its feeding of the 0^+ state could be removed. After correcting for the difference in the detection efficiencies for the two γ rays, it was found that about 8% of the events in the 1.022-MeV peak were due to feeding from the 2.15-MeV state.

In Fig. 1(b), the reconstructed ^{12}B excitation-energy spectra are shown, gated on the 0.718-MeV γ-ray peak (dashed red), which contains a mixture of $\Delta S = 0$ and $\Delta S = 1$ events, and on the 1.022-MeV γ-ray peak (solid black), which contains only $\Delta S = 0$ events. In both cases, backgrounds estimated in the sideband analysis are already subtracted, and in the case of the $\Delta S = 0$ spectrum, the contribution from feeding by the 2.15-MeV 1^+ state was also subtracted. The well-known strong Gamow-Teller ($\Delta S = 1$) transition ^{12}C(0^+, g.s.)$\rightarrow$^{12}B(1^+, g.s.) is clearly observed in the spectrum gated on the 0.718-MeV γ-ray. It is absent when the 1.022-MeV γ-ray gate is applied. Remaining events below 2 MeV in the latter spectrum are likely due to weak excitations of other low-lying states in ^{12}B. The disappearance of the transition to the ^{12}B ground state in the solid black spectrum shows that the $\Delta S = 0$ filter is effective. The broad peak around $E_x(^{12}\mathrm{B})$=9 MeV widens when gated on the 0.718-MeV peak. The reason is that in this spectrum (non-)spin-transfer dipole excitations to 0^-,1^-, and 2^- states contribute, whereas in the spectrum gated on the 1.022-MeV peak, only non-spin-transfer excitations to 1^- states contribute.

In Figs. 2(a-c), the measured double-differential cross sections for the ^{28}Si(^{10}Be,^{10}B) reaction are shown at three different center-of-mass (c.m.) scattering angles, gated on the ^{10}B($0_1{}^+$, 1.740 MeV)$\rightarrow$^{10}B($1_1{}^+$, 0.718 MeV) transition. The analysis was performed in an identical manner as for the ^{12}C target. Background contributions estimated by using the sideband and contribution from feeding through the ^{10}B($1_2{}^+$, 2.154 MeV)$\rightarrow$^{10}B($0_1{}^+$, 1.740 MeV) state have been subtracted from these spectra. Systematic uncertainties in the absolute normalization of the cross section are dominated by the uncertainty in the ^{10}Be beam intensity (4%)

To isolate the monopole ($\Delta L = 0$) contributions to the ^{28}Al excitation-energy spectrum, a MDA was performed [39, 40]. In the MDA, each 2-MeV wide bin in E$_x$(^{28}Al) was fitted with a linear combination of calculated angular distributions associated with ΔL = 0, 1, and 2. The calculated angular distributions were smeared to account for the experimental angular resolution prior to the fitting. Inclusion of angular distributions with ΔL >2, which peak at $\theta_{c.m.} > 2°$, did not improve the quality of the fits and did not alter the extracted contributions associated with the $\Delta L = 0$ and $\Delta L = 1$ excitations beyond statistical uncertainties. As an illustration of the MDA procedure, the differential cross sections and the MDA for the strong peak between $6 < E_x(^{28}\mathrm{Al}) < 12$ MeV and the range $18 < E_x(^{28}\mathrm{Al}) < 24$ MeV are shown in Figs. 2(d) and (e), respectively. Strong monopole and dipole contributions are present in Fig. 2(d). Fig. 2(e) also indicates a strong monopole contribution. The results from the MDA for the full excitation-energy range are shown in Figs. 2(a-c).

The angular distributions were calculated in distorted-wave Born approximation (DWBA) by using the code package `FOLD/DWHI` [41]. One-body transition densities (OBTDs) were calculated for the ^{10}Be-^{10}B system using `NUSHELLX@MSU` [42], and OBTDs for the ^{28}Si-^{28}Al system were obtained in the normal-modes (NM) formalism by using the code `NORMOD` [43]. In this formalism, 100% of the non-energy-weighted sum rule (NEWSR) associated with single-particle multipole operators is exhausted. The Love-Franey effective nucleon-nucleon (NN) interaction at 100 MeV [22] was used in the folding procedure.

The complex optical model potentials (OMPs) used to compute the ^{10}Be-^{28}Si entrance-channel and ^{10}B–^{28}Al exit-channel distorted waves were calculated by using the methods used routinely in the analysis of fast nucleon-removal reactions [44]. These employ the double-folding model [45], assuming ^{28}Si and ^{28}Al densities calculated from spherical Hartree-Fock (HF) calculations

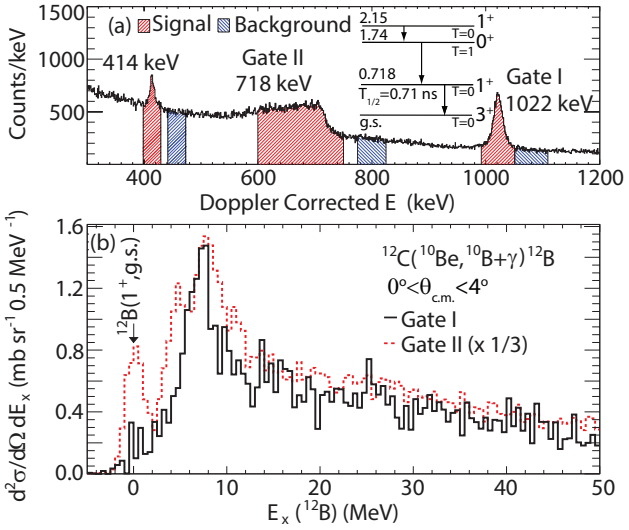

FIG. 1. (color online) (a) Doppler-reconstructed ($\beta = 0.43$) γ-ray spectrum from ^{12}C(^{10}Be,^{10}B+γ) reaction. The peak at 414 keV corresponds to ^{10}B($1_2{}^+$, 2.154 MeV)$\rightarrow$^{10}B($0_1{}^+$, 1.740 MeV). The peak at 718 keV (gate II) corresponds to ^{10}B($1_1{}^+$, 0.718 MeV)$\rightarrow$^{10}B($3_1{}^+$, *g.s.*). The peak at 1022 keV (gate I) corresponds to ^{10}B($0_1{}^+$, 1.740 MeV)$\rightarrow$^{10}B($1_1{}^+$, 0.718 MeV). (b) Side-band-subtracted double-differential cross sections gated on Gate I (solid black) and Gate II (dashed red).

using the SkX parametrization of the Skyrme interaction [46], Gaussian ^{10}Be and ^{10}B densities with root-mean-squared (rms) radii of 2.30 fm [47], and a Gaussian nucleon-nucleon NN effective interaction [48] with a range of 0.5 fm. Interaction strengths were taken from the tabulation of Ray [49].

The extracted monopole distribution at 0.25 ° from the MDA is shown in Fig. 3(a). It is attributed primarily to the excitation of the $2\hbar\omega$ IVGMR since there is no $0\hbar\omega$ excitation of the isobaric analog state for $N = Z$ nuclei. Two concentrations of strength are observed at ~ 9 and ~ 21 MeV. Monopole strengths observed above 35 MeV were consistent with 0, within uncertainties.

The extracted dipole distribution at 0.75° is shown in Fig. 3(b). It peaks at ~ 9 MeV and has a high-energy tail. This distribution is consistent with previous observations of the IVGDR in charge-exchange reactions with (n,p) [50] and (^{7}Li,^{7}Be) [51] probes and with observations of the analog transition in ^{28}Si through γ-absorption [52] and proton scattering [53]. The good agreement of the IVGDR distribution with previous data gives confidence in the reliability of the MDA shown in Fig. 2.

The blue-dashed curves in Fig. 3(a) and (b) indicate the differential cross sections associated with 100% exhaustion of the normal-modes NEWSR for the IVGMR (28.6 fm^4) and IVGDR (15.2 fm^2), respectively. The differential cross sections associated with full strength exhaustion drop with increasing excitation energies be-

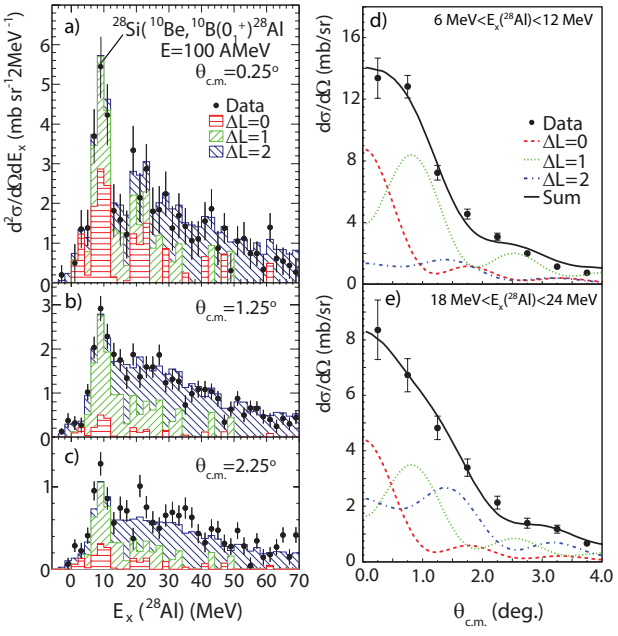

FIG. 2. (color online) (a-c) Double-differential cross sections for the ^{28}Si(^{10}Be,^{10}B*[1.74 MeV])^{28}Al reaction at three scattering angles, as indicated. The error bars on the data represent the statistical uncertainties. The colored histograms show the results of the MDA. (d) and (e) Differential cross sections and MDA analysis for the 6-12 MeV and 18-24 MeV ranges in the ^{28}Al spectrum, respectively.

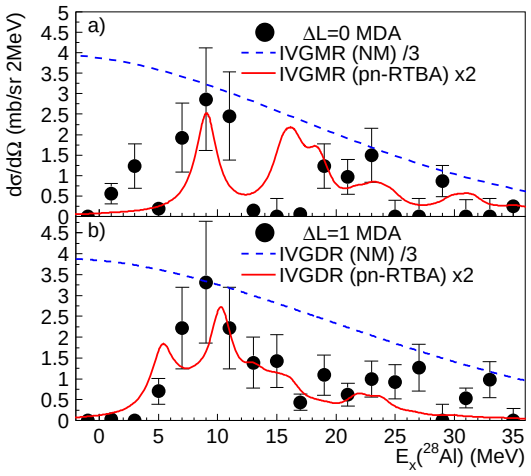

FIG. 3. (color online) (a) Differential cross sections extracted for monopole contributions to the ^{28}Al excitation-energy spectrum at 0.25° (black dots) are compared with NM calculations, i.e. for 100% of the NEWSR at each excitation energy (blue dashed line), and DWBA results based on pn-RTBA calculations (solid red line); see text for more details. Please note the scaling factors of 1/3 and 2 applied for the latter two, respectively. (b) Idem, but for the dipole cross sections at 0.75°.

cause of the increase in linear momentum transfer q. The red-solid curves represent the results based on the calculations in the proton-neutron relativistic time-blocking approximation (pn-RTBA) framework of Refs. [54, 55]. The pn-RTBA is an extension of time-dependent covariant density functional theory that includes particle-vibration coupling in the charge-exchange channel. Consequently, an improved description of the fragmentation of the strength is achieved [56] compared to earlier Hartree-Fock random-phase approximation calculations [5] for the IVGMR. The integrated strengths for the IVGMR (25.8 fm^4) and IVGDR (17.0 fm^2) in the pn-RTBA calculations are close to NM values. To convert the pn-RTBA strength distribution to the differential cross sections shown in Fig. 3(a) and (b), a proportional relationship between strength and peak differential cross section was assumed, based on the DWBA calculations using the NM OBTDs. Finally, the curves based on the pn-RTBA calculations were smeared with the experimental excitation-energy resolution.

The pn-RTBA calculations describe reasonably well the shape of the experimental distribution observed for the IVGDR, as shown in Fig. 3(b). However, the calculated cross sections are too low by about a factor of two: the measured cross sections represent 190(30)% the NEWSR for the IVGDR. Like the data, the pn-RTBA calculations for the IVGMR also display significant fragmentation. However, the detailed features of the experimental distribution are not as well reproduced as for the case of the IVGDR. This could be due to the fact that configurations beyond the $2p$-$2h$ are presently not

included in the pn-RTBA calculations. In addition, the calculations do not consider the considerable deformation of ^{28}Si [57]. As in the case of the IVGDR, the experimental cross section for the IVGMR is double the estimated cross section based on the pn-RTBA calculations: the measured cross sections represent 200(40)% of the NEWSR for the IVGMR. The discrepancy between the experimental and theoretical cross sections could be due to, or a combination of, deficiencies in the input of the DWBA calculations, such as the approximate treatment of the exchange contributions in the FOLD calculations [58], uncertainties in the strength of the τ component of the effective NN interaction, and uncertainties in the optical potential parameters. In addition, since heavy-ion CE reactions probe the nuclear surface and the τ component of the effective NN interaction is of very short range, the isovector non-spin-transfer cross sections are particularly sensitive to detailed features and variations of the transition densities near the surface. Hence, the assumed simple proportional relationship between transition strength and cross section, which has been well established for the $0\hbar\omega$ $\Delta L = 0$ transitions [1, 59, 60], could have large uncertainties for transitions with $\Delta L > 0$ and $2\hbar\omega$ excitations that have a node in the transition density near the surface.

We conclude that the (^{10}Be,^{10}B+γ[1022keV]) CE reaction at E(^{10}Be)=100 AMeV is a good tool for isolating isovector $\Delta S = 0$ excitations and a viable probe for studying the IVGMR, as evidenced by the successful extraction of IVGMR and IVGDR cross sections from reactions on ^{28}Si. The method will benefit from having ^{10}Be beams that are two or three orders of magnitude more intense so that heavier nuclei, in which the IVGMR excitation is more collective, can be studied in great detail. This can be achieved by performing experiments at one of the next-generation rare-isotope beam facilities or by producing a primary medium-energy ^{10}Be beam (its half-life is 1.51×10^6 years). In addition, by combining the results with data obtained with the (^{10}C,^{10}B+γ[1022keV]) reaction based on the same principle, it will be possible to evaluate the sum rule for the IVGMR. Improved beam intensities will also be very helpful for the development of more accurate reaction calculations for this new probe. It provides the prospect that calculations based on modern density-functional theories can be tested in more detail by comparing, in absolute terms, the exhaustion of transition strength.

We thank the staff at NSCL for their support. This work was supported by the US NSF [PHY- 1102511, PHY-1430152 (JINA Center for the Evolution of the Elements), PHY-1068217, PHY-1404442, PHY-1419765, and PHY-1404343]. GRETINA was funded by the US DOE Office of Science. Operation of the array at NSCL was supported by NSF under Cooperative Agreement PHY-11-02511 (NSCL) and DOE under grant DE-AC02-05CH11231 (LBNL). J.A.T. acknowledges support of the Science and Technology Facilities Council (UK) grant ST/L005743/1.

[1] M. N. Harakeh and A. van der Woude, *Giant Resonances: Fundamental High-Frequency Modes of Nuclear Excitation* (2001).
[2] N. K. Glendenning, Phys. Rev C **37**, 2733 (1988).
[3] J. M. Lattimer and M. Prakash, Phys. Rep. **333**, 121 (2000).
[4] G. Colò, Phys. Part. Nucl. **39**, 286 (2008).
[5] N. Auerbach and A. Klein, Nucl. Phys. **A395**, 77 (1983).
[6] G. Colò, M. Nagarajan, P. Van Isacker, and A. Vitturi, Phys. Rev. C **52**, R1175 (1995).
[7] J. D. Bowman, E. Lipparini, and S. Stringari, Phys. Lett. **197**, 497 (1987).
[8] P. Danielewicz, P. Singh, and J. Lee, Nucl. Phys. **A958**, 147 (2017).
[9] B. G. Todd-Rutel and J. Piekarewicz, Phys. Rev. Lett **95**, 122501 (2005).
[10] B. A. Brown, Phys. Rev. Lett. **85**, 5296 (2000).
[11] T. Suzuki, H. Sagawa, and G. Colò, Phys. Rev. C **54**, 2954 (1996).
[12] J. Jänecke, M. N. Harakeh, and S. Y. van der Werf, Nucl. Phys. **A463**, 571 (1987).
[13] I. Hamamoto and H. Sagawa, Phys. Rev. C **48**, R960 (1993).
[14] S. Fracasso and G. Colò, Phys. Rev C **72**, 064310 (2005).
[15] R. G. T. Zegers *et al.*, Phys. Rev. C **63**, 034613 (2001).
[16] D. Prout *et al.*, Phys. Rev. C **63**, 014603 (2000).
[17] J. Guillot *et al.*, Phys. Rev. C **73**, 014616 (2006).
[18] R. G. T. Zegers *et al.*, Phys. Rev. Lett. **90**, 202501 (2003).
[19] C. J. Guess *et al.*, Phys. Rev. C **83**, 064318 (2011).
[20] K. Miki *et al.*, Phys. Rev. Lett. **108**, 262503 (2012).
[21] W. G. Love and M. A. Franey, Phys. Rev. C **24**, 1073 (1981).
[22] M. A. Franey and W. G. Love, Phys. Rev. C **31**, 488 (1985).
[23] A. Erell *et al.*, Phys. Rev. Lett. **52**, 2134 (1984).
[24] A. Erell *et al.*, Phys. Rev. C **34**, 1822 (1986).
[25] F. Irom *et al.*, Phys. Rev. C **34**, 2231 (1986).
[26] S. Nakayama *et al.*, Phys. Rev. Lett. **83**, 690 (1999).
[27] N. Auerbach, F. Osterfeld, and T. Udagawa, Phys. Lett. **B219**, 184 (1989).
[28] N. Auerbach, Comm. Nucl. Part. Phys. **22**, 223 (1998).
[29] H. Lenske, H. H. Wolter, and H. G. Bohlen, Phys. Rev. Lett. **62**, 1457 (1989).
[30] Y. Sasamoto, *Study of the isovector non-spin-flip monopole resonance via the super-allowed Fermi type charge exchange (^{10}C,$^{10}B\gamma$) reaction*, dissertation, University of Tokyo (2012).
[31] S. Paschalis *et al.*, Nucl. Instr. Meth. Phys. Res. **A709**, 44 (2013).
[32] D. Weisshaar *et al.*, Nucl. Instrum. Meth. Phys. Res. B (2017), to be published.
[33] F. Marti, P. Miller, D. Poe, M. Steiner, J. Stetson, and X. Y. Wu, AIP Conf. Proc. **600**, 64 (2001).
[34] D. Morrissey, B. Sherrill, M. Steiner, A. Stolz, and I. Wiedenhoever, Nucl. Instr. Meth. Phys. Res. **B204**, 90 (2003).
[35] B. M. Sherrill *et al.*, Nucl. Instr. Meth. Phys. Res. **A432**, 299 (1999).
[36] D. Bazin, J. A. Caggiano, B. M. Sherrill, J. Yurkon, and A. Zeller, Nucl. Instr. Meth. Phys. Res. **B204**, 629

(2003).
[37] J. Yurkon *et al.*, Nucl. Instr. Meth. Phys. Res. **A422**, 291 (1999).
[38] D. R. Tiley *et al.*, Nucl. Phys. **A745**, 155 (2004).
[39] B. Bonin *et al.*, Nucl. Phys. **A430**, 349 (1984).
[40] T. Wakasa *et al.*, Phys. Rev. C **55**, 2909 (1997).
[41] J. Cook and J. Carr, computer program FOLD/DWHI, Florida State University (unpublished); based on F. Petrovich and D. Stanley, Nucl. Phys. **A275**, 487 (1977); modified as described in J. Cook *et al.*, Phys. Rev. C **30**, 1538 (1984); R. Zegers, S. Fracasso, and G. Colò, (unpublished).
[42] B. A. Brown and W. D. M. Rae, Nucl. Data Sheets **120**, 115 (2014).
[43] M. Hofstee *et al.*, Nucl. Phys. **A588**, 729 (1995); S. Y. van der Werf, computer code NORMOD, KVI Goningen, 1991 (unpublished).
[44] J. A. Tostevin and B. A. Brown, Phys. Rev. C **74**, 064604 (2006).
[45] J. A. Tostevin, (unpublished), computer codes FRONTHF and SMATPOT.
[46] B. A. Brown, Phys. Rev. C **58**, 220 (1998).
[47] A. Ozawa *et al.*, Nucl. Phys. **A691**, 599 (2001).
[48] J. A. Tostevin, J. Phys. G **25**, 735 (1999).
[49] L. Ray, Phys. Rev. C **20**, 1857 (1979).
[50] J. Ullmann *et al.*, Nucl. Phys. **A386**, 179 (1982).
[51] S. Nakayama *et al.*, Phys. Lett. **B195**, 316 (1987).
[52] H. Harada *et al.*, J. Nucl. Sci. Tech. **38**, 465 (2001).
[53] R. Fea *et al.*, arXiv:1409.1080 [nucl-ex].
[54] T. Marketin *et al.*, Phys. Lett. **B706**, 477 (2012).
[55] E. Litvinova *et al.*, Phys. Lett. **B730**, 307 (2014).
[56] C. Robin and E. Litvinova, Eur. Phys. J. A **52**, 205 (2016).
[57] P. Möller, A. Sierk, T. Ichikawa, and H. Sagawa, Atomic Data and Nuclear Data Tables **109110**, 1 (2016).
[58] G. Perdikakis *et al.*, Phys. Rev. C **83**, 054614 (2011).
[59] T. Taddeucci *et al.*, Nucl. Phys. **A469**, 125 (1987).
[60] F. Osterfeld, Rev. Mod. Phys. **64**, 491 (1992), and refereces therein.